Tech. Note ARDB 231

A New Lithium Oven Plasma Source For E-157 Plasma Wakefield Accelerator Experiments

K. A. Marsh and Shuoqin Wang

INTRODUCTION

A new 1.4 meter long lithium oven has been built for the recent E-157 Plasma Wakefield Accelerator Experiment. The construction and operation is similar to that of the oven described in [1]. Based on the need for more accurate characterization of the lithium oven plasma source, there are some new diagnostic features for the present oven. Internal thermocouple probes were installed along the oven for monitoring the spatial profile of the lithium temperature. White light absorption, to measure the lithium neutral density, has been calibrated against Hook interferometry for several oven operating conditions.

The organization of this paper is as follows. In the first section, we briefly introduce the new features of the oven. We present the temperature distribution along the oven with different helium buffer pressure and heating power. The results show the main characteristics of the oven mode. In the second section, we verify indirectly that temperatures measured by the inner thermocouples are the vapor temperatures. Based on the vapor pressure curve P(T), the vapor density distribution is then deduced, which characterizes the oven length quantitatively. In the third section, we describe

white light absorption measurements. All theories predict that the linewidth due to self-broadening should be proportional to the neutral density. However, there is up to two times difference in the constant of proportionality among the published theoretical results. We find the value of the constant, for which the neutral density deduced from the white light absorption measurement agrees well with the hook measurement. In the forth section, we discuss how to manipulate the UV laser profiles to produce a uniform plasma. The plasma density distribution is given.

Section 1 Features of the new 1.4 meter lithium vapor source

The description and performance of the prototype of the heat pipe oven has been introduced in [1]. So the details of the heat pipe oven such as the scheme and the description of the oven, the formation of the vapor zone, the function of the metal mesh, buffer gas, the definition of oven mode, etc are ignored here. There are four thermocouples embedded inside the oven. The thermocouple locations are indicated in Figure 1. The results show the oven temperature distribution with and without Li. Also the oven profile is more uniform when operated at higher temperatures and pressures. A long thermocouple probe was pulled through the center of the oven to confirm the profile in Figure 1. We have the following results shown in Figure 1 and 2.

Section 2 Vapor density from vapor-pressure curve and its comparison with hook measurement

In principle, the temperature detected by the inside thermocouples can be regarded as the vapor temperature if the effect of longitudinal vapor flow can be ignored [2]. We find it to be reasonable assumption based on our

oven parameters and has been justified by the following measurement. We deduce the vapor density distribution along the oven by referring to the vapor-pressure curve [3]. The optical length ∫ndl can be calculated numerically and then compared with the result from hook method. The result is shown in the Figure 3.

The measurements of optical lengths from two methods under different buffer pressures are summarized in Figure 4.

Optical length ∫ndl measured by hook method can be accurate enough down to 6% uncertainty. The uncertainty is due to the systematic errors in the hook method itself. ∫ndl deduced from vapor pressure curve has a 5% uncertainty due to the limited temperature measurement along the oven. We conclude from the above data that temperatures measured from thermocouples are the vapor temperatures. The longitudinal vapor flow can be ignored until the vapor reaches the ends of the oven. We acquire Figure 5 of vapor density distribution along the oven, based on the temperature measurement under different buffer pressure and the vapor-pressure curve.

From the above density distribution, oven length can be defined quantitatively. In Table 1, we show the buffer pressure, the readout of the inner temperature, and heat power that leads to a 1.4 meter long column of lithium.

Pressure (mTorr)	T1 (degree)	T2	T3	T4	Hook nL (10^{17}cm^{-2})	Vapor Density (10^{15}cm^{-3})	Current (Amp)
443	673.97	699.3	704.7	706.4	7.04	5.04	7.1
400	637	692	699.5	701.4	6.47	4.6	7.04
351	640.4	685.5	692.7	695.5	5.65	4.13	6.97
300	636.8	679.8	687.1	691.3	5.22	3.82	6.98
250	607.9	665.6	676.3	681.6	4.2	3.18	6.8
204	601.8	658.3	669.1	676.6	4.04	2.88	6.8

Table 1 working condition for different vapor density requirement

Note that in a later setup, a stainless steel cover was installed on the outside of the oven bricks. This made the oven heater more efficient and so less heater power (or current) was needed to produce the same results in Table 1.

Section 3 White light absorption measurement and its comparison with hook measurement

We have mainly used hook method and white light absorption method to test the new heat pipe oven. The detailed schemes of both of the methods have been introduced in [1].

Hook measurement, based on the disperse or imaginary part of the refractive index, is generally more accurate than absorption measurement, since it is not sensitive to the linewidth of the absorbing transition [4]. However, due to its complication and fragility of the experimental system, hook method cannot be set up at the beam line in the harsh environment. The white light absorption method measures the absorption coefficient, which is the function of the vapor density. The function itself is sensitive to the linewidth, and therefore less accurate. In white light absorption measurement, we have

$$I = I_0 \cdot e^{-\alpha \cdot L}$$

$$. \alpha = \frac{0.5 n_{vapor} \cdot r_0 \cdot f \cdot \Delta\nu}{(\nu - \nu_0)^2 + (\frac{\Delta\nu}{2})^2} \qquad (1)$$

α is the absorption coefficient, ν_0 is the resonance frequency, $\Delta\nu$ is linewidth. r_0 is the classical radius, and f is the oscillator strength The linewith $\Delta\nu$ is a complicated function of n_{vapor} since there several mechanisms that contribute to linewidth broadening, such as Stark broadening (i.e., foreign gas pressure broadening), Doppler broadening, self-broadening, natural linewidth, etc [5]. However, based on the parameters of lithium vapor we are working on, such as vapor temperature, vapor pressure and helium buffer pressure, etc. self-broadening dominate over natural linewidth and Stark broadening [6] . Doppler broadening can be ignored if numerical fit is only applied to the Lorentzian wings of the absorption curve[7].

Theory predicts that $\Delta\nu_{SB}$ is proportional to n_{vapor}, which has

$$\Delta\nu_{SB} = K\frac{r_0 \cdot f \cdot n_{vapor}}{\nu_0} \qquad (2)$$

The constant of proportionality K depends on the assumptions and techniques of the theoretical calculation. The published values vary by a factor of two, i.e., K=1, 0.585, 1.047, 1.333 [8,9,10,11]. We use each of them in our following analysis and compare the value of n_{vapor} to hook measurement.

Sustituting Eq.(2) to Eq(1) to form an equation with vapor density as one parameter to be fit, We analyze the experimental curve far away from the absorption center with nonlinear least square fitting routine and find the best-fit vapor density. An example of curve-fit is shown in the Figure 6.

We compare the vapor density derived from the above method and hook method shown in Figure 7.

We conclude that white light absorption measurement agrees with Hook measurement quite well if K=1.333 is used.

Section 4 Plasma production

In E-157, plasma is produced when 193nm ArF excimer laser photons shine through Lithium vapor source and photoionize Li atoms. UV laser energy is attenuated according to

$$E(z) = E_0 e^{-n_{vapor}\sigma z} \qquad (3)$$

σ is the photoionization cross-section of the Li atom, which is about $1.8*10^{-18}$ cm^{-2}. Here it is assumed that UV laser energy attenuation is solely due to the photoionization of one electron of a Li atom. Therefore, plasma production satisfies that

$$dE(z) = -h\nu \cdot n_e(z) \cdot S(z) \cdot dz \qquad (4)$$

and

$$n_e(z) = \frac{n_0 \sigma}{h\nu} \frac{E(z)}{S(z)} \qquad (5)$$

S(z) is the laser beam size. It can be seen from (5) that:

(1) Plasma density n_e is proportional to laser intensity.

(2) The uniformity of plasma depends on the uniformity of the laser intensity. In other words, the beam profile S(z) has to be manipulated to compensate the attenuation of E(z).

For instance, Figure 8 shows Li vapor density distribution along the oven. If we can focus the laser beam size as in Figure 9, then we can have a uniform plasma density distribution as in Figure 10.

During the experimental run, the actual plasma profile and density will depend on laser performance and focusing setup.

Section 5 Conclusion

The oven and plasma parameters are fundamental to the analysis of the experimental results of E-157. The oven described here was used during the run of May 2000. The oven parameters were monitored continuously during the run. White light absorption was successfully used on line to confirm the desired oven density.

REFERENCES

[1] P. Muggli et al., " Photo-Ionized Lithium Source for Plasma Accelerator Application, " IEEE Transactions on Plasma Science, vol. 27, no. 3, pp 791, June 1999.

[2] C. R. Vidal, " Spectroscopic observations of subsonic and sonic vapor flow inside an open-ended heat pipe, " J. Appl. Phys., vol. 44, no. 5, pp 2225, May 1973.

[3] V. S. Yargin, " Transport properties of saturated lithium vapor, " Inzh.-Fiz. Zh., no. 3, pp 494, 1992.

[4] W. C. Marlow, " Hakenmethode, " Appl. Opt., vol. 6, no. 10, pp 1715, 1967.

[5] H. L. Chen, "Applications of laser absorption spectroscopy, " Laser Spectroscopy and its applications, edited by Radziemski et al., pp 261, 1987.

[6] R. B. Miles et al., " Optical third-harmonic generation in alkali metal vapors, " IEEE J.QE, vol. QE-9, no. 4, pp470, April 1973.

[7] A. E. Siegman, " Lasers, " pp172, University Science Books, 1986.

[8] V. F. Weisskopf, Z. Physik 75, 287, 1932.

[9] W. W. Houston, " Resonance broadening of spectral lines, " Phys. Rev., vol. 54, pp. 884, 1938.

[10] H. Margenau et al., Rev. Mod. Phys., 8, 22, 1936.

[11] W. Furssow, et al., Physik. Z. Sowjetunion, 10, 378, 1936.

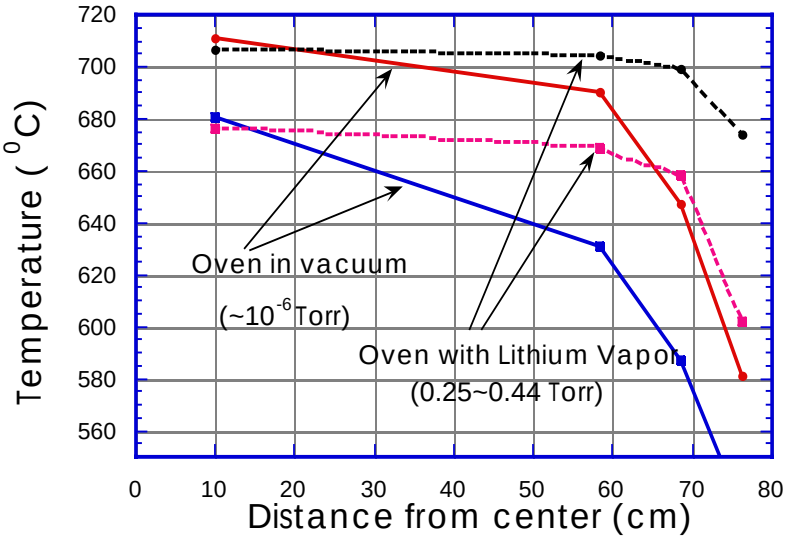

Figure 1 Temperature distribution with and without lithium for different heater powers.

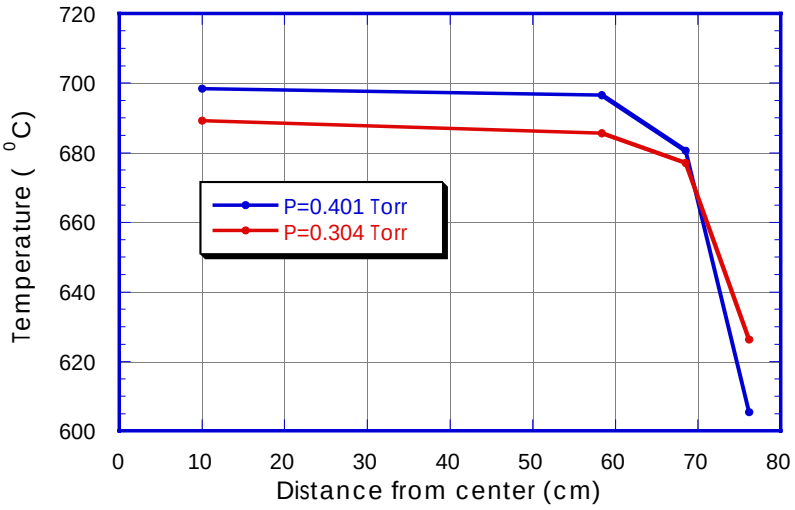

Figure 2 Temperature distribution with the same power as the helium buffer pressure goes up. It shows clearly the characteristics of oven mode, where the buffer pressure controls the vapor density.

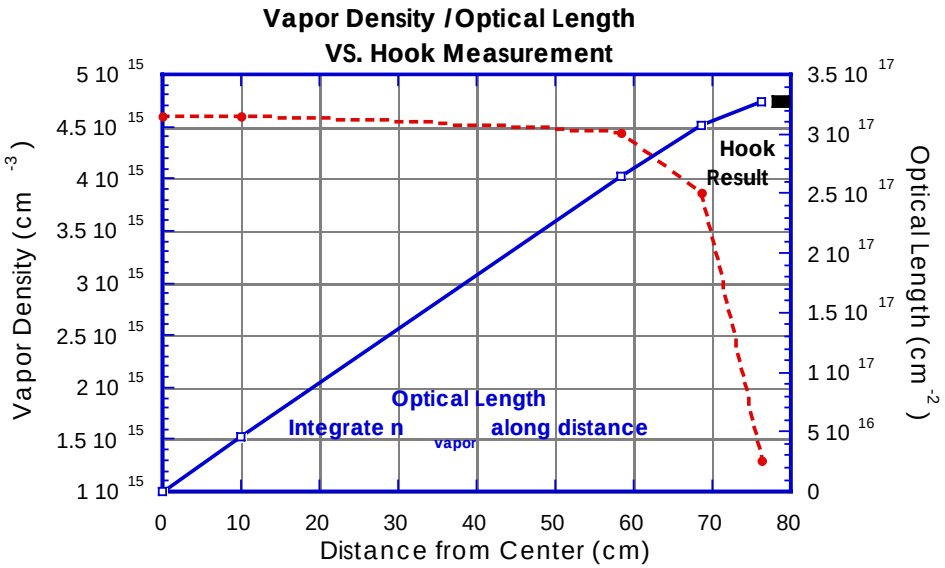

Figure 3 vapor densities are deduced from the vapor pressure curve based on the temperatures provided by thermal couples. Optical length is the integral of vapor densities along the oven. The result then compares with that from hook method. (The experimental data shown in the figure is taken at 0.4 Torr buffer pressure.) Notice that only half of the oven distance is considered in the optical length integration.

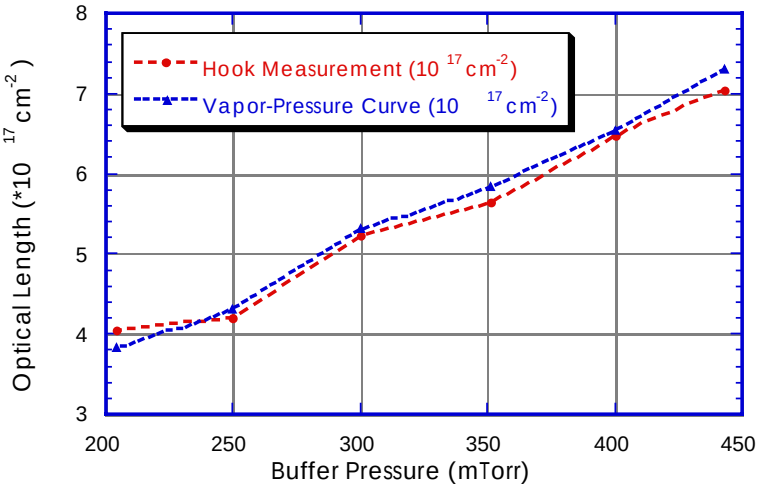

Figure 4 Under different pressure, The value of optical lengths are also measured by hook method and deduced from vapor pressure curve.

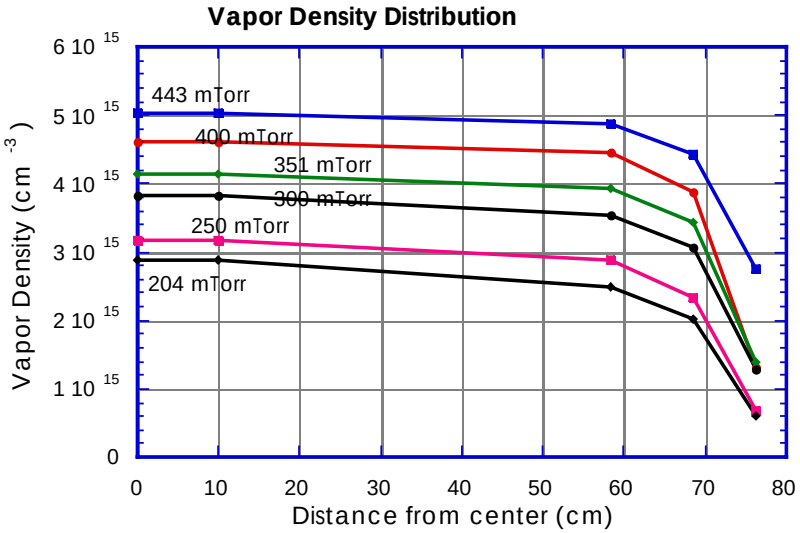

Figure 5 Density distribution along the oven under different buffer pressure.

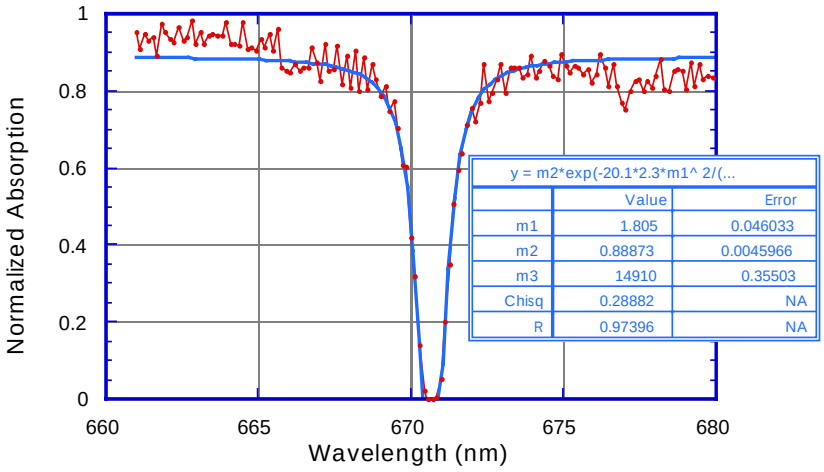

Figure 6 There are three to-be-fit parameters. m1 is neutral density in the unit of (*$10^{15}$$cm^{-3}$). m2 is the normalized factor, m3 is the absorption center in unit of (cm^{-1}).

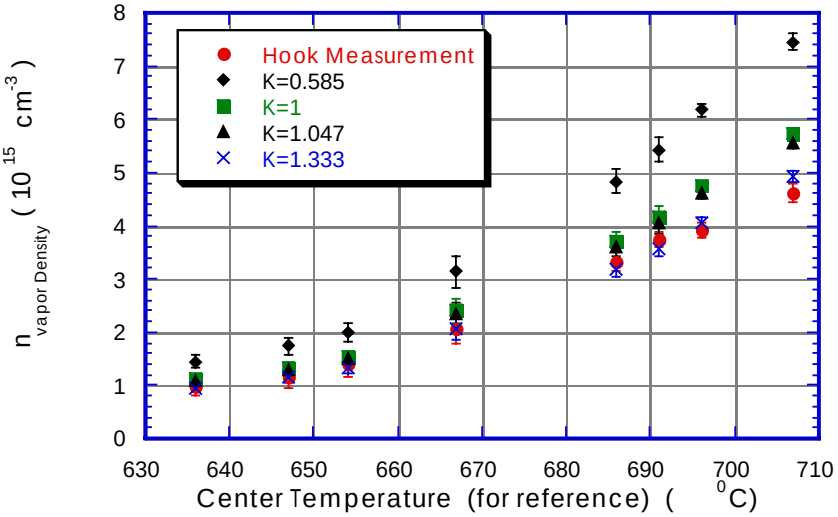

Figure 7 Vapor density is measured by both hook method and white light absorption method. Constant K in four different values is used in the curve-fit analysis.

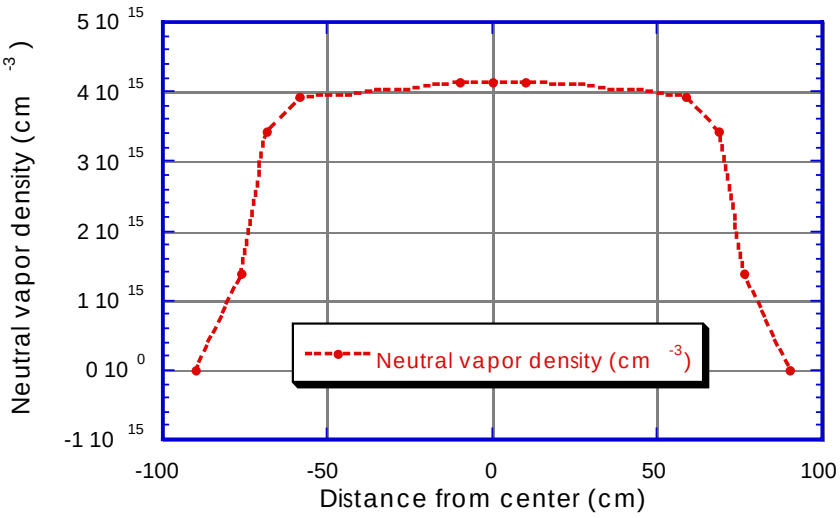

Figure 8 Vapor density distribution along the oven with the buffer pressure 351 mTorr.

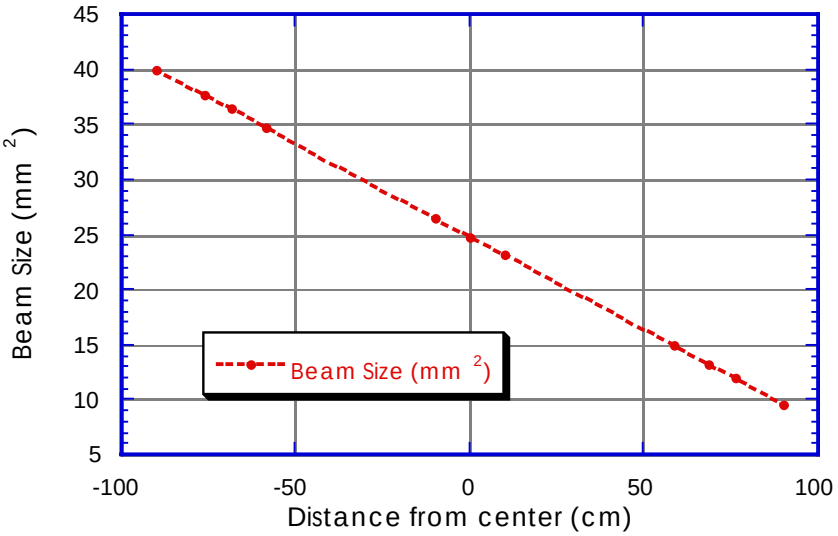

Figure 9 Beam size is focused along the oven ideally.

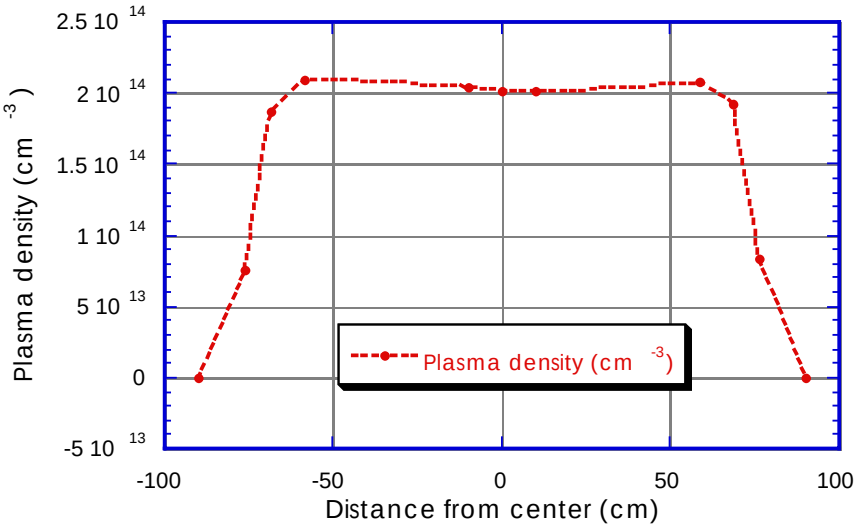

Figure 10 Plasma density production along the oven based the measured neutral density distribution and the idealized beam profiles.